THE JOURNAL OF BIOLOGICAL CHEMISTRY
Vol. 277, No. 14, Issue of April 5, pp. 12061–12066, 2002

Printed in U.S.A.

Folding of Dimeric Methionine Adenosyltransferase III

IDENTIFICATION OF TWO FOLDING INTERMEDIATES*

Received for publication, December 4, 2001, and in revised form, January 25, 2002
Published, JBC Papers in Press, January 28, 2002, DOI 10.1074/jbc.M111546200

Manuel M. Sánchez del Pino‡§, Isabel Pérez-Mato¶, Jesús M. Sanz‖, José M. Mato, and Fernando J. Corrales‡

From the Division of Hepatology and Gene Therapy, University of Navarra, Irunlarrea 1, 31008 Pamplona, Spain and the ‖Centro de Biología Molecular y Celular, University Miguel Hernández, Av. Ferrocarril s/n, 03202 Elche (Alicante), Spain

Methionine adenosyl transferase (MAT) is an essential enzyme that synthesizes AdoMet. The liver-specific MAT isoform, MAT III, is a homodimer of a 43.7-kDa subunit that organizes in three nonsequential α-β domains. Although MAT III structure has been recently resolved, little is known about its folding mechanism. Equilibrium unfolding and refolding of MAT III, and the monomeric mutant R265H, have been monitored using different physical parameters. Tryptophanyl fluorescence showed a three-state folding mechanism. The first unfolding step was a folding/association process as indicated by its dependence on protein concentration. The monomeric folding intermediate produced was the predominant species between 1.5 and 3 M urea. It had a relatively compact conformation with tryptophan residues and hydrophobic surfaces occluded from the solvent, although its N-terminal region may be very unstructured. The second unfolding step monitored the denaturation of the intermediate. Refolding of the intermediate showed first order kinetics, indicating the presence of a kinetic intermediate within the folding/association transition. Its presence was confirmed by measuring the 1,8-anilinonaphtalene-8-sulfonic acid binding in the presence of tripolyphosphate. We propose that the folding rate-limiting step is the formation of an intermediate, probably a structured monomer with exposed hydrophobic surfaces, that rapidly associates to form dimeric MAT III.

The classical investigation of Anfinsen and co-workers (1) demonstrates that the sequence of amino acids that comprise a polypeptide encodes the information required to reach the correct three-dimensional fold of a protein. However, the mechanism by which the amino acid sequence directs the folding of a protein is still unknown. Typically, protein folding studies have concentrated on small, single domain proteins that fold rapidly and avoid aggregation (2–4). However, in living cells, most proteins have more than 100 residues with multiple folding domains and subunits. These large proteins are not likely to follow all of the folding principles established for smaller proteins. They probably have more complex folding rules so that models based on studies of small globular proteins may not fully explain their folding and assembly (5). Folding of multidomain or multisubunit proteins usually involves the formation of partially folded intermediates. Although the basic principles governing protein folding are probably general, folding of oligomeric proteins may be a two-state process or involve monomeric or multimeric intermediates (6–9). Additionally, association may occur from completely folded monomers (10–13), or alternatively, final folding steps occur after association of partially folded subunits (14). All these different mechanisms make it difficult to derive a global mechanism to describe the folding of oligomeric proteins, and consequently each protein must be studied individually. Defining the complete folding pathway requires the identification and characterization of all stable and transient conformational states that exist along the folding and unfolding pathways.

S-Adenosylmethionine (AdoMet)[1] is an essential metabolite in all cells. AdoMet is the most important biological methyl group donor and is a precursor in the synthesis of polyamines (15–17). Additionally, it has been recently demonstrated that reduction of AdoMet levels in liver is associated with liver injury and hepatocarcinoma (18). Methionine adenosyltransferase (MAT) (EC 2.5.1.6) catalyzes the only known AdoMet biosynthetic reaction (19, 20). In all organisms studied so far, from *Escherichia coli* to humans, sequence homologies show that MAT is an exceptionally well conserved enzyme through evolution (17). In mammalian tissues three different forms of MAT (MAT I, MAT III, and MAT II) have been identified that are the product of two different genes (*MAT1A* and *MAT2A*, respectively) (21–25). The gene *MAT2A* encodes a 396-amino acid catalytic subunit (α_2) expressed in all mammalian tissues (16, 26). MAT II consist of α_2 catalytic and β regulatory subunits, although the stoichiometry of the oligomer has not been yet established. The gene *MAT1A* is expressed mainly in adult liver and encodes a 395-amino acid catalytic subunit (α_1) that organizes in dimers, MAT III, and tetramers, MAT I (17, 20). The reason for the presence of these two different isoenzymes in liver has not been yet elucidated, although it may be an adaptation to the metabolic requirements of the liver. The liver has the highest specific activity of MAT, which agrees with the observation that up to 85% of all methylation reactions and as much as 50% of methionine catabolism occur in this tissue (27,

* This work was supported by Grants SAF 98/0132 and SAF 99/0038 from the Comisión Interministerial de Ciencia y Tecnología and by grants from Europharma, Knoll and Fundación Aguas de Valencia. The costs of publication of this article were defrayed in part by the payment of page charges. This article must therefore be hereby marked "*advertisement*" in accordance with 18 U.S.C. Section 1734 solely to indicate this fact.

‡ To whom correspondence may be addressed: Division of Hepatology and Gene Therapy, University of Navarra, Irunlarrea 1, 31008 Pamplona (Navarra), Spain. Tel.: 34-948-425678; Fax: 34-948-425677; E-mail: fjcorrales@unav.es or mspino@unav.es.

§ Supported by a Contrato de reincorporación from the Spanish Ministerio de Educación y Cultura.

¶ Supported by a Beca Formación de Personal Investigador from the Spanish Ministerio de Educación y Cultura.

[1] The abbreviations used are: AdoMet, *S*-adenosylmethionine; ANS, 1,8-anilinonaphtalene-8-sulfonic acid; MAT, methionine adenosyltransferase; MALDI-TOF, matrix-assisted laser desorption/ionization-time of flight.

28). Based upon the different kinetic properties of MAT I and MAT III isoforms, MAT III has been considered the liver-specific enzyme. While MAT I, similar to MAT II in extrahepatic tissues, may maintain the basal AdoMet levels required by cells, MAT III would be responsible for the clearance of methionine after a load of this amino acid. *E. coli* and liver MAT have been crystallized and their structure solved, showing that the tetramer structure of both enzymes is essentially the same (29–31). Each subunit consists of three structural domains related to each other by a pseudo 3-fold symmetry. Pairs of subunits form dimers, and each dimer is a tight complex, with a wide interface area between subunits, that accommodate two active sites (29–31). The active site of the enzyme is made by both subunits. However, no information about the folding mechanism of MAT is still available. We have characterized the folding-assembly pathway of MAT III, the specific liver isoform, by identifying the intermediates involved in the process. Our kinetic and equilibrium experiments indicate that the folding of MAT III involves the formation of two folding intermediates, which were identified by their intrinsic fluorescence, ANS binding capacity, and hydrodynamic volume.

EXPERIMENTAL PROCEDURES

Materials—Columns and chromatography media were from Amersham Biosciences. Urea was from Invitrogen. All other reagents were from Sigma.

Site-directed Mutagenesis—A 1.2-kilobase fragment containing the rat *MAT1A* coding region (32) was subcloned into a pET vector. The resulting plasmid includes a 5′ sequence that encodes for 6 histidine residues and a thrombin cleavage site in-frame with the rat liver *MAT1A* coding region. Mutants were obtained by inverse polymerase chain reaction according to the procedure of Pérez-Mato *et al.* (33). Mutants were identified by sequencing the complete MAT cDNA.

Expression and Purification of His-tagged MAT I/III R265H Mutant—MAT I/III R265H mutant was overexpressed in *E. coli* BL21(DE3) as previously described (33). Recombinant MAT I/III R265H mutant protein was purified from the bacterial cytosolic extracts by affinity chromatography on a Ni^{2+}-Sepharose column equilibrated in 50 mM Tris/HCl, pH 8, 0.5 M NaCl, 75 mM imidazole following the procedures described by Pérez-Mato *et al.* (33). No changes in the fluorescence, CD spectra, oligomeric state, and enzymatic activity were observed after digestion of the recombinant proteins with thrombin (data not shown). Therefore all the assays were carried out using the His-tagged recombinant proteins.

Purification of MAT from Rat Liver—MAT III was purified from rat liver according to the procedure described previously (34). Protein purity was more than 95% as estimated by SDS-PAGE (35).

Size Exclusion Chromatography—Protein samples (4.6 μM) were analyzed using a Superdex 200 HR 10/30 column equilibrated with 50 mM Tris/HCl, pH 7.5, 150 mM KCl, 10 mM $MgCl_2$ in an AKTA FPLC (Amersham Biosciences). After sample injection (100 μl), proteins were isocratically eluted at a flow rate of 0.8 ml/min. Protein elution was monitored by the absorbance at 280 nm. The elution volumes (ml) of the standard proteins were: thyroglobulin (669 kDa), 8.1; ferritin (440 kDa), 10.22; catalase (232 kDa), 12.11; ovoalbumin (43 kDa), 14.73; chymotrypsin A (25 kDa), 18; ribonuclease A (13.7 kDa), 19. According to the elution volume of the standard proteins, the estimated molecular masses of native rat liver MAT III and R265H MAT I/III mutant were 90 and 41 kDa, respectively.

Equilibrium Denaturation Experiments—The buffer composition in all equilibrium experiments was 50 mM Tris/HCl, pH 8, 4 mM $MgCl_2$, 150 mM KCl, and 3.6 mM dithiothreitol with different urea concentrations. All experiments were performed at 25 °C with the protein concentration indicated in the figure legends and incubated in the presence of urea for at least 2 h. Unfolding was monitored by recording the fluorescence emission spectra at each urea concentration from 300 to 450 nm emission wavelength using an excitation wavelength of 280 nm in a PerkinElmer LS50B luminescence spectrometer. An emission wavelength of 321 nm is used in all plots, because this is the wavelength where differences were maximal. After recording the emission spectra, ANS was added from a 1 mM stock solution to make a final concentration of 10 μM. When required, tripolyphosphate/magnesium from a stock of 50 mM was added to make a final concentration of 500 μM. The fluorescence at 470 nm emission wavelength was recorded in both cases using an excitation wavelength of 350 nm. When unfolding was monitored by measuring the tripolyphosphatase activity, MAT III was incubated for 2 h at 25 °C in 990 μl of the above buffer. After this time, the reaction was started by addition of 10 μl of tripolyphosphate/magnesium to make the final concentration 2 mM. At different incubation times, aliquots of 100 μl were removed to determine the formation of inorganic phosphate according to the method of Lanzetta (36). For refolding experiments MAT III was unfolded in the same buffer with a final urea concentration of 8 M. After 2 h at 25 °C refolding was started by diluting unfolded MAT III 20 times to obtain the desired urea concentrations. Refolding proceeded for 2 additional hours. Fluorescence values were normalized by the protein concentration and expressed as arbitrary units per nanomolar MAT III monomers. Enzyme activity was expressed as min^{-1}.

Refolding Kinetic Experiments—MAT III was partially unfolded for 2 h at 25 °C in the same buffer indicated above with a final urea concentration ranging from 1.4 to 2.6 M. Refolding was started by a 1/10 dilution of the MAT III solution to obtain a final urea concentration of 0.26 M. Intrinsic fluorescence was monitored using excitation and emission wavelengths of 280 and 321 nm, respectively. When ANS binding was monitored all solutions contained 10 μM ANS, and refolding was monitored using an excitation wavelength of 350 nm and an emission wavelength of 470 nm. The approximate dead time was about 10 s.

Limited Proteolysis and Mass Spectrometry Analysis—Limited proteolysis was performed by incubation of MAT III (0.5 mg/ml) with trypsin (0.01 mg/ml) in 10 mM ammonium bicarbonate, pH 8, at 25 °C for different periods of time. Protein fragments were analyzed by SDS-PAGE. Mass spectrometry analysis was carried out with a Micromass MALDI-TOF spectrometer. After digestion, reaction mixture was 5-fold diluted with 0.1% trifluoroacetic acid and then spotted (1.5 μl) onto the MALDI target, where it was mixed with an equal volume of matrix (cinnaminic acid). The analysis was performed using a laser energy of 70%, and M_r was calculated using adenocorticotropic hormone and trypsin autolysis fragments as near point and internal standards, respectively.

Data Analysis—Equilibrium experiments were all fitted to a three-state model with a folding/association step and an additional folding step (Equation 1). As discussed below, the folding intermediate is assumed to be monomeric.

$$N_2 \overset{K_1}{\longleftrightarrow} 2I \overset{K_2}{\longleftrightarrow} 2U \qquad \text{(Eq. 1)}$$

where N, I, and U are native, intermediate, and unfolded protein, respectively. K_1 and K_2 are the equilibrium constants for the folding/association and folding steps, respectively. If the species present at each urea concentration are expressed as fraction (f), then the conservation of mass and the equilibrium constants can be expressed as follows,

$$f_N + f_I + f_U = 1 \qquad \text{(Eq. 2)}$$

$$K_1 = \frac{2f_I^2 P}{f_N};\ K_2 = \frac{f_U}{f_I} \qquad \text{(Eq. 3)}$$

where P is the total concentration of MAT III subunits. From Equations 2 and 3, and solving for the fraction of each species we get the following equation.

$$f_I = \frac{K_1(1+K_2)}{4P}\left(-1 + \sqrt{1 + \frac{8P}{K_1(1+K_2)^2}}\right);$$

$$f_N = 1 - f_I(1+K_2);\ f_U = f_I K_2 \qquad \text{(Eq. 4)}$$

The dependence of the equilibrium constants on the denaturant (D) concentration can be obtained form the free energy of unfolding ΔG_u

$$\Delta G_u = -RT \ln K_u = \Delta G_u^{H_2O} - m[D] \qquad \text{(Eq. 5)}$$

where $\Delta G_u^{H_2O}$ is the free energy of unfolding in water, and m is the coefficient of dependence on the denaturant concentration.

The measured signals (S_D) depend on the species composition at each urea concentration according to the following equation,

$$S_D = S_N f_N + S_I f_I + S_U f_U \qquad \text{(Eq. 6)}$$

where S_N, S_I, and S_U are the specific signal of native, intermediate, and unfolded protein, respectively.

The equilibrium experiments were fitted in the spreadsheet Microsoft Excel as follows. The equilibrium constants K_1 and K_2 were

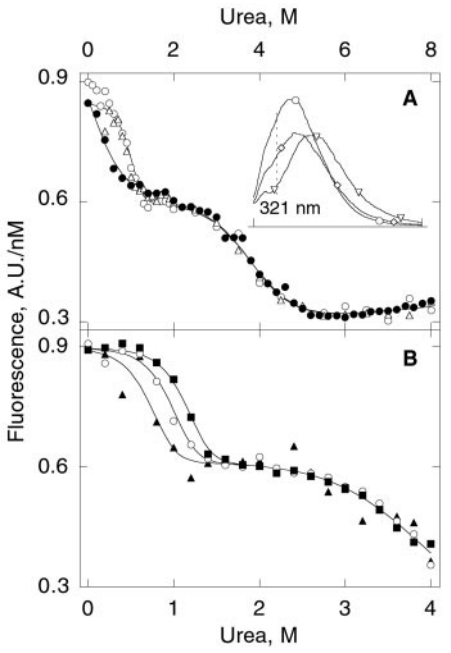

FIG. 1. **Intrinsic fluorescence.** Unfolding and refolding of MAT III was monitored by measuring the fluorescence at 321 nm at 25 °C as described under "Experimental Procedures." *A*, unfolding of MAT III (○) and monomeric mutant R265H (●) was performed using a subunit protein concentration of 280 nM. Refolding of MAT III (△) was also monitored. *Inset*, fluorescence spectra of MAT III at different urea concentrations: 0 M (○), 2 M (◇), and 6 M (▽). *B*, unfolding of MAT III was monitored at different subunit protein concentrations: 29 nM (▲), 290 nM (○), and 1.48 μM (■). The *solid lines* represent the fit to Equation 6 performed as described under "Experimental Procedures." The fitting parameters are indicated in Table I.

TABLE I
Fitting parameters

Thermodynamic parameters				
Transition	Protein	m	$\Delta G_u^{H_2O}$	$D_{0.5}$
		kcal mol^{-1} *M*$^{-1}$	*kcal mol*$^{-1}$	*M*
1st	R265H	1.31	−0.09	−0.07
1st	wt[a]	5.55	6.12	1.10
2nd	Both	1.15	4.41	3.82

Global conformational stability		
	wt	R265H
ΔG_u (kcal mol^{-1})	14.93	4.32

Physicochemical parameters					
Parameter	Protein	Fig.	N	I	U
Intrinsic fluorescence	wt	1*A*	0.84	0.60	0.32
	R265H	1*A*	1.16		
	wt	1*B*	0.89	0.61	0.22
ANS fluorescence	wt	2*A*	0.52	0.09	0.03
	wt	2*B*	0.50	0.09	−0.01
Activity	wt	2*A*	3.60	0.17	−0.13
Elution volume	wt	3	14.25	14.38	13.07
	R265H	3	15.31	14.36	13.10

Kinetic parameters			
Urea	[MAT]	Amplitude	k
M	*nM*	*AU/nM*	*min*$^{-1}$
2.3	29.6	0.162	0.27
2.3	296	0.227	0.27
2.3	2960	0.178	0.24
1.4	296	0.169	0.23
2.0	296	0.184	0.20
2.3	296	0.168	0.21
2.6	296	0.183	0.22

[a] wt, wild type.

calculated for each denaturant concentration using initial estimate values of $\Delta G_u^{H_2O}$ and m. Then, the fraction of each species was calculated using Equation 4. The specific signal of each species was then calculated as the regression coefficients of the fraction of the species in a multiple linear regression analysis between the calculated fractions and the measured signals at all urea concentrations, using a built-in function of the program. This is like solving Equation 6 for all urea concentrations. The theoretical signal was then calculated using Equation 6. The agreement between calculated and measured signal was then evaluated by least square. Changing only $\Delta G_u^{H_2O}$ and m using an iterative procedure (quasi-Newton method) obtained the best fit. In this way, all the different types of signals measured could be fitted simultaneously to the same folding mechanism with only two variables per transition. When several conditions were evaluate at the same time, such as unfolding and refolding or different protein concentrations, average specific signals were used to calculate the theoretical signal. Sometimes the specific signal appeared to depend on the denaturant concentration. In such cases, a slope was introduced in the fitting process.

Kinetic data were fitted to single first or second order rate equations,

$$S(t) = S_\infty + Ae^{-kt} \quad \text{(Eq. 7)}$$

$$S(t) = S_\infty + \frac{A}{1 + Pkt} \quad \text{(Eq. 8)}$$

where $S(t)$ is the signal recorded at time t, $S\infty$ is the signal at $t = \infty$, A is the amplitude of the signal, and k is the rate constant.

RESULTS

Intrinsic Fluorescence—The equilibrium unfolding and refolding in the presence of urea was monitored by changes in the intrinsic fluorescence of MAT III at 321 nm (Fig. 1*A*). The unfolding of MAT III was a completely reversible process with two transitions. The initial drop in fluorescence was the result of a decrease in intensity, whereas the second one reflected a red shift of the spectrum without a significant change in fluorescence intensity (*inset* in Fig. 1). These data indicate the presence of a stable folding intermediate whose tryptophan residues are still buried within the protein. The midpoints for the transitions were 1.10 and 3.82 M urea using 0.28 μM MAT III monomer (see thermodynamic parameters in Table I).

Equilibrium experiments performed with the mutant R265H, which is a monomer (37), also showed two transitions (Fig. 1*A*). The first transition took place at a lower urea concentration compare with wild type MAT III, whereas the second transition paralleled the one observed at 3.82 M urea. This result suggests that both proteins unfold via the same folding intermediate.

The second transition, corresponding to the unfolding of the intermediate, must be a unimolecular process, since the R265H mutant is a monomer. Thus, we studied the protein concentration dependence of the first transition. As shown in Fig. 1*B*, the transition was shifted toward higher urea concentrations with increasing MAT III concentrations. This result suggests that the transition observed at about 1 M urea represents the folding/association process between native MAT III and a stable intermediate.

Enzyme Activity and ANS Binding—Equilibrium experiments were also monitored by measuring tripolyphosphatase activity as well as ANS binding capacity. Both parameters showed a single transition at about 1 M urea (Fig. 2*A*). ANS binds to large patches of hydrophobic surface exposed to solvent and has been widely used to probe folding intermediates. However, ANS seemed to bind the native conformation of the enzyme rather than the intermediate. We have determined an apparent binding stoichiometry of 1 mol of ANS per MAT III subunit (not shown), suggesting that ANS binds to a specific site. Recently, the crystal structure of ANS bound to a single site of a protein has been solved (38). A similar environment

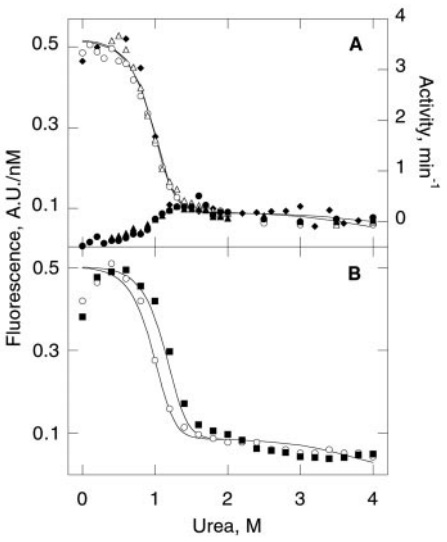

FIG. 2. **ANS binding.** Unfolding and refolding of MAT III was monitored by its ANS binding capacity as well as by its tripolyphosphatase activity as described under "Experimental Procedures." *A*, ANS fluorescence during unfolding, in the absence (○) and in the presence of tripolyphosphate (●), and refolding, in the absence (△) and in the presence of tripolyphosphate (▲), of MAT III using a subunit protein concentration of 280 nM. The tripolyphosphatase activity during unfolding (♦) was also monitored using a subunit protein concentration of 296 nM. *B*, ANS fluorescence during unfolding of MAT III was monitored at different subunit protein concentrations: 290 nM (○) and 1.48 μM (■). The *solid lines* represent the fit to Equation 6 performed as described under "Experimental Procedures." The fitting parameters are indicated in Table I.

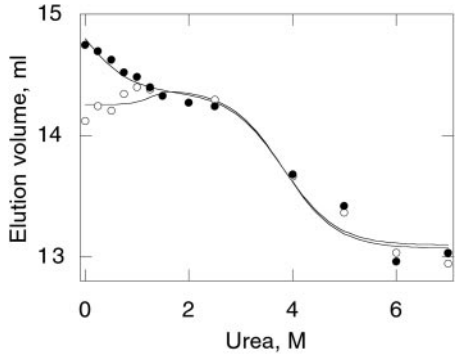

FIG. 3. **Hydrodynamic volume.** The compactness of the species present at different urea concentrations was studied by gel filtration chromatography using a subunit protein concentration of 4.6 μM. The elution volume of MAT III (○) and the R265H mutant (●) at different urea concentrations is represented. The *solid lines* represent the fit to Equation 6 performed as described under "Experimental Procedures." The fitting parameters are indicated in Table I.

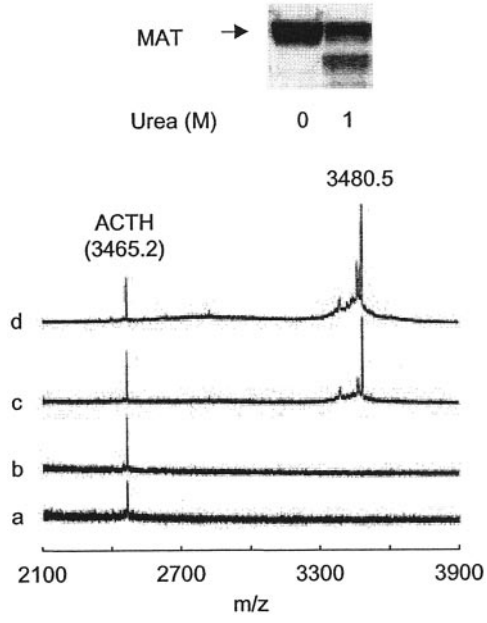

FIG. 4. **Trypsin accessibility of MAT III folding intermediate.** Limited proteolysis experiments were performed in the absence and in the presence of 1 M urea as described under "Experimental Procedures." The protein subunit concentration was 11.4 μM. Protein fragments were analyzed by SDS-PAGE (*top panel*). The formation of the complementary fragment from MAT III trypsin digestion as well as its M_r was determined by MALDI-TOF mass spectrometry analysis (*bottom panel*). MAT III was incubated in the absence of urea for 60 min (*trace a*) or in the presence of 1 M urea for 0 (*trace b*), 30 (*trace c*), and 60 (*trace d*) min.

was found in the MAT III structure at the entrance of substrates to the active site. Supporting the existence of such a binding site was the quenching of the fluorescence signal produced by the addition of the substrates of the enzyme (Fig. 2*A*). Thus, enzyme activity and ANS binding are both probably probing the conformation of the same structural domain of the protein. This would explain the parallel loss of activity and ANS binding upon unfolding of the native protein.

Hydrodynamic Volume—The compactness of the species present at different urea concentrations was studied by gel filtration chromatography. In the absence of urea the elution volume of MAT III and R265H mutant corresponded to that of dimeric (14.3 ml) and monomeric (15.3 ml) forms, respectively (Fig. 3). However, as the urea concentration increased the elution volume of both proteins became closer until reaching the same intermediate value (14.4 ml) at about 1.25 M urea. At higher urea concentrations the decrease in elution volume was the same for MAT III and R265H mutant until reaching the value of unfolded monomer (13.1 ml). These data also support the presence of a common folding intermediate in the unfolding pathway of both proteins. This folding intermediate had a less compact structure than the monomer as indicated by its larger hydrodynamic volume.

Trypsin Accessibility—To gain information about the conformation of the folding intermediate, limited proteolysis experiments were performed. In the absence of urea MAT III was resistant to cleavage by trypsin for 1 h at 25 °C (Fig. 4). However, in the presence of 1 M urea, a single proteolytic fragment was detected by SDS-PAGE. It was estimated to have about 3 kDa less than native MAT III. This is consistent with a single cleavage either at the N- or C-terminal end of the protein. The mass of the complementary fragment, as determined by mass spectrometry, was 3480.5 Da, which is consistent with a cleavage at the N-terminal side of lysine 33. This residue is located near the interacting interface between subunits. Thus, in order for this residue to become accessible to trypsin, a monomeric intermediate should be present.

Refolding Kinetics—To further characterize the transition between native MAT III and its folding intermediate, the refolding kinetics was monitored by changes in fluorescence intensity at 321 nm. To study the protein concentration dependence, different concentrations of MAT III (from 0.3 to 30 μM) were incubated at 2.3 M urea. Under these conditions the folding intermediate represented over 95% of the protein. Refolding was started upon a 1/10 dilution. The same refolding kinetics was observed at all MAT III concentrations. Moreover, the data could be fitted to a single exponential but was poorly described by a second order rate equation, indicating that the traces shown in Fig. 5 corresponded to monomolecular reactions. Similar results were obtained when refolding was monitored by ANS binding (not shown). These results imply that in

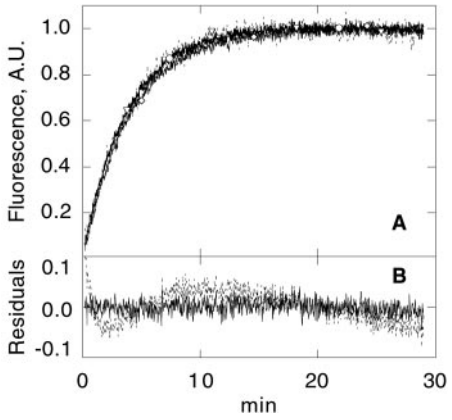

FIG. 5. **Refolding kinetics.** Refolding of MAT III was monitored by recording the fluorescence at 321 nm. *A*, different subunit protein concentrations were used: 29.6 nM (◇, *dashed line*), 296 nM (○, *thick line*), and 2.96 μM (▽, *thin line*). The data were fitted to a first or second order rate equation as described under "Experimental Procedures." The fitting parameters are indicated in Table I. Normalized traces are shown. *B*, residuals of the fit of the 296 nM trace to a first (*continuous line*) or second order (*dashed line*) rate equation.

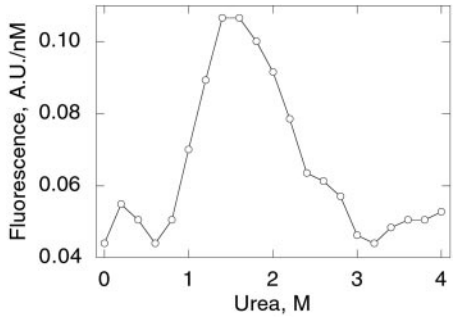

FIG. 6. **Kinetic folding intermediate.** MAT III was incubated at different urea concentrations in the presence of 10 μM ANS and 500 μM tripolyphosphate as described under "Experimental Procedures." The protein subunit concentration was 1.48 μM.

the folding pathway from the stable intermediate to the native protein there must be at least one kinetic folding intermediate. In an attempt to obtain some physical evidence of the existence of this intermediate, we measured the binding of ANS in the presence of tripolyphosphate using a MAT III concentration of 1.48 μM. Fig. 6 shows a transient binding of ANS within the transition observed at about 1 M urea, indicating the presence of the intermediate. However, when refolding started from urea concentrations ranging from 1.4 to 2.6 M, the same kinetics, with no significant loss of amplitude, were observed (Table I). These results suggest that it is a folding intermediate that is not significantly populated in our equilibrium experiments. However, it must bind a large amount of ANS nonspecifically in order to be detected.

DISCUSSION

The overall unfolding pathway for a dimeric protein must begin with the folded dimer (N_2) and end with two unfolded monomers (2U). The way in which this process occurs depends on whether intermediates are present along the pathway. Numerous examples exist of compact monomeric or dimeric intermediates that are significantly populated during the equilibrium denaturation of a folded dimer (6–9). However, far from being a general mechanism, the formation and role of these intermediates needs to be addressed in light of the protein under investigation. Here we describe the folding mechanism of MAT III, the liver isoform of a ubiquitous enzyme that synthesizes AdoMet. MAT III is a homodimer of a 43.7-kDa subunit (17, 20) that organizes in three nonsequential α-β domains (29–31). Although the MAT III structure has been recently resolved, little is known about its folding mechanism.

All our results from equilibrium experiments have been fitted to the following folding scheme,

$$2U \xleftarrow{\text{folding}} 2I \xleftarrow{\text{folding/association}} N_2$$

SCHEME 1

where U, I, and N denote unfolded, intermediate, and native protein, respectively.

Unfolding of MAT III is a reversible process with formation of a stable monomeric folding intermediate. A fully reversible three-state folding process was observed when unfolding was monitored by fluorescence, indicating the presence of a stable folding intermediate. Gel filtration experiments also supported these results. On the contrary, only a single transition, corresponding to the formation of the intermediate, was observed by measuring tripolyphosphatase activity or ANS binding. The folding intermediate was the predominant species between 1.5 and 3 M urea. Unfolding of the mutant R265H also showed a three-state folding mechanism. The second transition of both proteins, corresponding to the unfolding of the intermediate, was identical, which strongly suggests that they both unfold via the same folding intermediate. Since R265H is a monomeric mutant (37) (and it is involved only in monomolecular reactions, not shown), the folding intermediate must also be a monomer. The first transition observed in the case of the mutant protein, however, took place at a lower urea concentration, indicating that the monomeric mutant is less stable than dimeric MAT III at the same protein concentration. Moreover, even in the absence of urea, the R265H mutant seemed to be in equilibrium with the folding intermediate, because no plateau was observed.

The stable folding intermediate may be a molten globule. The physicochemical properties of the folding intermediate are similar to those proposed for the molten globule (39). It has an intermediate compactness as indicated by its hydrodynamic volume, which is larger than the monomer, but much smaller than the unfolded protein. Its fluorescence spectrum indicated that tryptophan fluorescence was quenched (compare with native protein). However, tryptophan residues did not seem to be exposed to the solvent, because the emission maximum was the same as in the native protein. After its unfolding, a red shift of the spectrum was observed, indicating their exposure to the media. The folding intermediate was inactive and unable to bind ANS specifically (see below). There were no hydrophobic patches exposed to the solvent, because it did not bind ANS, indicating that the dimerization interface was not accessible. Lysine 33 is located more or less in the middle of the dimerization interface with its side chain buried within the protein. Thus, to be accessible to trypsin digestion the folding intermediate must be a monomer with the dimerization interface completely altered. This lysine residue appeared to be the most sensitive toward trypsin cleavage, even more than lysine residues at the surface of the protein, which suggests that the N-terminal region might be extended.

There is a specific binding site for ANS that may be located near the access to the active site. The apparent binding stoichiometry of 1 mol of ANS per MAT III subunit suggests that ANS binds to a specific binding site. Recently, the crystal structure of a binding site for ANS has been described (38). ANS is stacked in a hydrophobic cleft made by the sequence Pro-Gly at one side and the hydrophobic side chain of an arginine at the other side. A similar environment is also found in MAT III. The only Pro-Gly sequence in MAT III is located opposed to the hydrophobic side chains of Val-Gly-Ala. This last

sequence is at the beginning of the loop that limits the access to the active site of the enzyme and that is probably involved in catalysis (40). The quenching of ANS fluorescence after addition of substrates supports the location of this putative binding site. Moreover, the loss of activity paralleled the quenching of ANS fluorescence, suggesting that they are probing the same structural domain of the protein.

There is a kinetic intermediate between native protein and the stable folding intermediate. The first transition, at about 1 M urea, was dependent on protein concentration. This implies a folding/association reaction, because the folding intermediate is a monomer. However, refolding kinetics only showed a first order process, which can only be explained by the presence of a kinetic intermediate. This kinetic intermediate could be monomeric or dimeric. If a dimeric intermediate was present, all of the following conditions should be met: 1) the spectroscopic properties of the dimeric intermediate should be identical to that of the monomeric folding intermediate so that there is no loss of amplitude; 2) formation of the intermediate should be much faster than subsequent monomolecular steps. It should be completed within the dead time (about 10 s) of our experiments, otherwise a protein concentration-dependent lag phase should be present; 3) the kinetic intermediate should accumulate within the dead time. However, our data do not support all these requirements. Whereas the first requirement might be true for intrinsic fluorescence, it did not seem to hold for fluorescence due to ANS binding (Fig. 6). Then, accumulation of the kinetic intermediate would produce different kinetics (with losses of amplitude) when monitored by tryptophan or ANS fluorescence. Thus, the kinetic intermediate is most probably a monomer. There are several possibilities regarding the spectroscopic properties and the rate-limiting step. However, the simplest mechanism that explains our data with the minimum number of assumptions is a monomeric intermediate with spectroscopic properties (at least intrinsic fluorescence) like those of the native protein and whose formation (the folding step) is rate-limiting. Thus, no protein-dependent lag phases nor losses of amplitude, which were not seen, should be expected. It could be speculated that this kinetic intermediate would be the folded or very structured monomer. Thus, exposure of the large hydrophobic dimer interface would be energetically unfavorable so that association is expected to be very fast, maybe diffusion-controlled. This would also explain the high nonspecific binding of ANS of the intermediate.

We propose that both MAT III and the R265H mutant would share the two folding intermediates described here. However, once the kinetic folding intermediate would be formed the folding pathways of both proteins would diverge. In the case of MAT III, association of two monomers would take place rapidly. Since association is impaired in the case of the R265H mutant, an alternative, more compact monomeric conformation would be produced. This conformation would presumably occlude the mainly hydrophobic interface between subunits to stabilize a monomeric conformation.

In summary, our results indicate that MAT III unfolding is fully reversible with the following proposed folding mechanism,

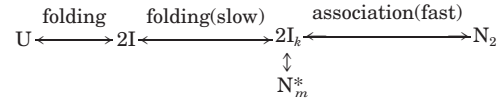

SCHEME 2

where U, I, and N denote unfolded, intermediate, and native protein, respectively, and the subscript *k* indicates that it is a kinetic intermediate. The subscript *m* and the asterisk indicate that it is a monomeric mutant with an altered native-like conformation. The stable monomeric folding intermediate has an altered non-native dimerization interface with no exposure of hydrophobic patches or tryptophan residues to the solvent. Although it is less compact than native MAT III, it is much more compact than unfolded protein. The kinetic intermediate present in the transition between the stable folding intermediate and native MAT III is most probably a monomer whose formation is rate-limiting and associates very rapidly to form native MAT III. The monomeric mutant R265H unfolds via the same stable folding and, probably, kinetic intermediates. Our data also indicate that ANS binds MAT III specifically at a site that is probably located near the access to the active site.

REFERENCES

1. Anfinsen, C. B. (1973) *Science* **181,** 223–230
2. Creighton, T. E. (1990) *Biochem. J.* **270,** 1–16
3. Jaenicke, R. (1991) *Biochemistry* **30,** 3147–3161
4. Serrano, L., Kellis, J. T., Jr., Cann, P., Matouschek, A., and Fersht, A. R. (1992) *J. Mol. Biol.* **224,** 783–804
5. Neet, K. E., and Timm, D. E. (1994) *Protein Sci.* **3,** 2167–2174
6. Clark, A. C., Sinclair, J. F., and Baldwin, T. O. (1993) *J. Biol. Chem.* **268,** 10773–10779
7. Doyle, S. M., Braswell, E. H., and Teschke, C. M. (2000) *Biochemistry* **39,** 11667–11676
8. Jaenicke, R., and Lilie, H. (2000) *Adv. Protein Chem.* **53,** 329–401
9. Blackburn, M., and Noltman, E. (1981) *Arch. Biochem. Biophys.* **212,** 162–169
10. Waddle, J. J., Johnston, T. C., and Baldwin, T. O. (1987) *Biochemistry* **26,** 4917–4921
11. Ziegler, M. M., Goldberg, M. E., Chaffotte, A. F., and Baldwin, T. O. (1993) *J. Biol. Chem.* **268,** 10760–10765
12. Goldenberg, D. P., and King, J. (1981) *J. Mol. Biol.* **145,** 633–651
13. Haase-Pettingell, C., and King, J. (1997) *J. Mol. Biol.* **267,** 88–102
14. Jaenicke, R., and Rudolph, R. (1989) in *Protein Structure: A Practical Approach* (Creighton, T. E., ed) IRL Press (Oxford University, Press) Oxford
15. Cantoni, G. L. (1975) *Annu. Rev. Biochem.* **44,** 435–441
16. Kotb, M., and Geller, A. M. (1993) *Pharmacol. Ther.* **59,** 125–143
17. Mato, J. M., Alvarez, L., Ortiz, P., and Pajares, M. A. (1997) *Pharmacol. Ther.* **73,** 265–280
18. Mato, J. M., Corrales, F. J., Lu, S. C., and Avila, M. A. (2001) *FASEB J.* **16,** 15–26
19. Cantoni, G. (1953) *J. Biol. Chem.* **204,** 403–416
20. Kotb, M., Mudd, S. H., Mato, J. M., Geller, A. M., Kredich, N. M., Chou, J. Y., and Cantoni, G. L. (1997) *Trends Genet.* **13,** 51–52
21. Okada, G., Teraoka, H., and Tsukada, K. (1981) *Biochemistry* **20,** 934–940
22. Sullivan, D. M., and Hoffman, J. L. (1983) *Biochemistry* **22,** 1636–1641
23. Kotb, M., and Kredich, N. M. (1985) *J. Biol. Chem.* **260,** 3923–3930
24. Cabrero, C., Puerta, J., and Alemany, S. (1987) *Eur. J. Biochem.* **170,** 299–304
25. Hoffman, J. L. (1983) *Methods Enzymol.* **94,** 223–228
26. Mitsui, K., Teraoka, H., and Tsukada, K. (1988) *J. Biol. Chem.* **263,** 11211–11216
27. Mudd, S. H., and Poole, J. R. (1975) *Metabolism* **29,** 707–720
28. Finkelstein, J. D. (1990) *J. Nutr. Biochem.* **1,** 228–237
29. Takusagawa, F., Kamitori, S., and Markham, G. D. (1996) *Biochemistry* **35,** 2586–2596
30. Takusagawa, F., Kamitori, S., Misaki, S., and Markham, G. D. (1996) *J. Biol. Chem.* **271,** 136–147
31. González, B., Pajares, M. A., Hermoso, J. A., Alvarez, L., Garrido, F., Sufrin, J. R., and Sánchez-Aparicio, J. (2000) *J. Mol. Biol.* **300,** 363–375
32. Mingorance, J., Alvarez, L., Sanchez-Gongora, E., Mato, J. M., and Pajares, M. A. (1996) *Biochem. J.* **315,** 761–766
33. Pérez-Mato, I., Castro, C., Ruiz, F. A., Corrales, F. J., and Mato, J. M. (1999) *J. Biol. Chem.* **274,** 17075–17080
34. Sánchez del Pino, M. M., Corrales, F. J., and Mato, J. M. (2000) *J. Biol. Chem.* **275,** 23476–23482
35. Laemmli, U. K. (1970) *Nature* **227,** 680–685
36. Lanzetta, P. A., Alvarez, L. J., Reinach, P. S., and Candia, O. A. (1979) *Anal. Biochem.* **100,** 95–97
37. Mato, I. P., Sánchez del Pino, M. M., Chamberlin, M. E., Mudd, S. H., Mato, J. M., and Corrales, F. J. (2001) *J. Biol. Chem.* **276,** 13803–13809
38. Schonbrunn, E., Eschenburg, S., Luger, K., Kabsch, W., and Amrhein, N. (2000) *Proc. Natl. Acad. Sci. U. S. A.* **97,** 6345–6349
39. Ptitsyn, O. B. (1992) in *Protein Folding* (Creighton, T. E., ed) pp. 243–300, Freeman & Co., New York
40. Fu, Z., Hu, Y., Markham, G. D., and Takusagawa, F. (1996) *J. Biomol. Struct.*